

Matter-wave entanglement and teleportation by molecular dissociation and collisions

T. Opatrný¹ and G. Kurizki

Department of Chemical Physics, Weizmann Institute of Science, 761 00 Rehovot, Israel

¹*Theor. Phys. Institut, F. Schiller Universität, Max-Wien-Platz 1, D-07743 Jena, Germany*
and Theor. Phys. Dept., Palacký University, Svobody 26, 77146 Olomouc, Czech Republic

(November 9, 2018)

We propose dissociation of cold diatomic molecules as a source of atom pairs with highly correlated (entangled) positions and momenta, approximating the original quantum state introduced by Einstein, Podolsky and Rosen (EPR) [Phys. Rev. **47**, 777 (1935)]. Wavepacket teleportation is shown to be achievable by its collision with one of the EPR correlated atoms and manipulation of the other atom in the pair.

03.67.Hk, 03.65.Ud, 39.20.+q

The fundamentally profound notion of quantum teleportation is the prescription of how to map, in a *one to one fashion*, any quantum state of system A onto that of a *distant* system B: one must measure the pertinent observables of A, then manipulate their counterparts in B according to the communicated results of the measurements on A [1–7]. Teleportation has thus far been explored for photon polarizations [1–4], optical field quadratures [5,6] and multi-atom spin components [7]. Here we pose the basic question: How to teleport the *translational quantum states (wavepackets) of material bodies* over sizeable distances? We propose dissociation of cold diatomic molecules as a source of atom pairs with highly correlated (entangled) positions and momenta, approximating the original quantum state introduced by Einstein, Podolsky and Rosen (EPR) [8]. Wavepacket teleportation [2] is shown to be achievable by its collision with one of the EPR correlated atoms and manipulation of the other atom in the pair.

Consider a cold beam of ionized molecules that are moving with high, constant velocity v_z along the z -axis (which thus *plays the role of time*) to a region where they are dissociated by means of an electromagnetic pulse. Let the size L of the dissociation region along the perpendicular x -axis be defined by means of an aperture (Fig. 1). Here the molecule splits and its two constituents start receding.

In order to be coherent within the dissociation region L , the translational *center-of-mass* (COM) state of the molecule along the x -axis should be close to the minimum uncertainty state (MUS) of its position and momentum, described by a Gaussian $\exp[-P_x^2/2\Delta P_x^2]$, where P_x is the x -component of the COM momentum and ΔP_x its spread. Such a state can be prepared by translationally cooling the molecules to the ground state of a trapping potential, then ionizing and accelerating them to the re-

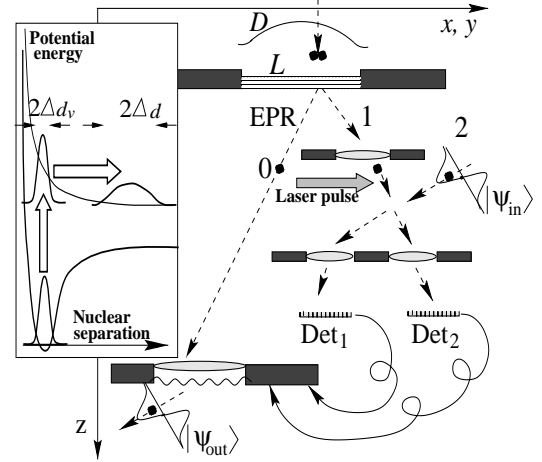


FIG. 1. EPR entanglement and teleportation of atomic wavepackets. A cold diatomic with COM spread D dissociates into translationally entangled atoms or ions 0 and 1. Particle 1 is focussed and laser-deflected to collide with particle 2. Their post-collision distance and momentum-sum are measured by detectors 1 and 2 and determine the position and momentum shifts of particle 0, whose translational state $|\psi_{\text{out}}\rangle$ then approximately reproduces $|\psi_{\text{in}}\rangle$ of particle 2. Inset: short-pulse dissociation yields a replica of the internuclear wavepacket on the dissociative potential surface, whose gradient causes the wavepacket to spread.

quired speed v_z (prior to dissociation). The required temperature is typically $T \approx \hbar^2/(Mk_B D^2)$, where M is the molecular mass, k_B is the Boltzmann constant and D , the COM wavepacket size, is chosen to be $D \lesssim L$. A size $D \approx 300$ nm would require $T \approx 3$ μK for H_2^+ and $T \approx 0.4$ μK for Li_2^+ . Such temperatures are achievable by Raman photoassociation of atomic pairs in Bose condensates [9].

We would like the two-atom translational state obtained by molecular dissociation to closely resemble the *original* EPR state [8], whose realization has not been investigated thus far. The perfect EPR state of particles 0 and 1 is described by the wavefunction $\Psi(x_0, x_1) = \delta(x_0 - x_1)$: the positions and momenta of the two particles along x are completely uncertain, yet perfectly correlated (entangled): $x_0 = x_1$, $p_{x0} = -p_{x1}$. The resemblance of the dissociated state to the perfect EPR state depends on the extent to which the variances of the correlated atomic variables are *below* the Heisenberg uncer-

tainty limit, so that

$$\Delta x_{01} \Delta P_x \ll \hbar, \quad (1)$$

$\hat{x}_{01} = \hat{x}_0 - \hat{x}_1$ and $\hat{P}_x = \hat{p}_{x_0} + \hat{p}_{x_1}$ being respectively the internuclear separation and COM momentum operators. Inequality (1) is possible since the two variances *do not* pertain to canonically conjugate variables. The diatomic molecule prior to dissociation is describable by an internuclear wavepacket whose spatial size is Δd_v (typically 0.1 nm), determined by its vibrational state. Dissociation by a short laser pulse can yield an *almost exact replica* of the initial internuclear wavepacket on a dissociative electronic potential surface of the molecule (Fig. 1-inset). The much broader, cold COM wavepacket keeps during dissociation the molecular MUS spread (Fig. 1) $\Delta P_x \approx \hbar/D$. As the internuclear wavepacket *becomes nearly free* shortly after dissociation, it may still resemble an EPR state. Its proximity to the perfect EPR state at $t = 0$, chosen to signify the *completion* of dissociation, can be measured by the parameter s that is inversely proportional to the left-hand side of (1)

$$s \approx D/\Delta d. \quad (2)$$

Here the width $\Delta d = \Delta x_{01}(0) > \Delta d_v$ is determined by the dynamical spreading of the internuclear wavepacket, caused by the gradient of the dissociative potential surface. The ratio in (2) should be sought to satisfy $s \gg 1$, in accordance with inequality (1), the perfect EPR state having $s \rightarrow \infty$. Even for the realistic values $\Delta d \sim 1 \text{ nm} \gg \Delta d_v$, and $D \gtrsim 300 \text{ nm}$, this parameter is remarkably large: $s \approx 300$.

There is a noteworthy analogy between the two-particle EPR state and that of entangled two-mode light from parametric downconversion (PDC) [10,11]: s is analogous to the exponential of the “squeezing parameter” of such light, which represents the ratio of the standard deviation of the “stretched” field quadrature to that of its “squeezed” counterpart (one quadrature corresponding, e.g., to the sum and the other to the difference of the two fields, analogously to our \hat{x}_{01} and \hbar/\hat{P}_x , respectively). In current optical experiments [11] $s \lesssim 4$.

Outside the dissociation region (typically, for separations beyond a few nm) the receding particles evolve freely, with diminishing position correlation. Yet the two-particle wavefunction remains inseparable, having the form $\Psi(x_0, x_1) = \psi(x_{01})\psi_{\text{COM}}(x_0 + x_1)$, i.e., a product of the internuclear wavefunction and its COM counterpart. The spread of the coordinate difference x_{01} then grows with time as $\Delta x_{01}^2(t) = \Delta d^2 + \Delta v_{01}^2 t^2$, Δv_{01} being the spread of their velocity difference acquired during dissociation (here we assume homonuclear diatomic molecules, for simplicity). Yet the growth of $\Delta x_{01}(t)$ *can be compensated* by a suitable lens, which *ideally* “time-reverses” Δx_{01} , i.e., projects it back to its initial “spot” of size $\Delta x_{01}(0) = \Delta d$. In practice, such compensation is limited by the resolution of the focussing lens (see below).

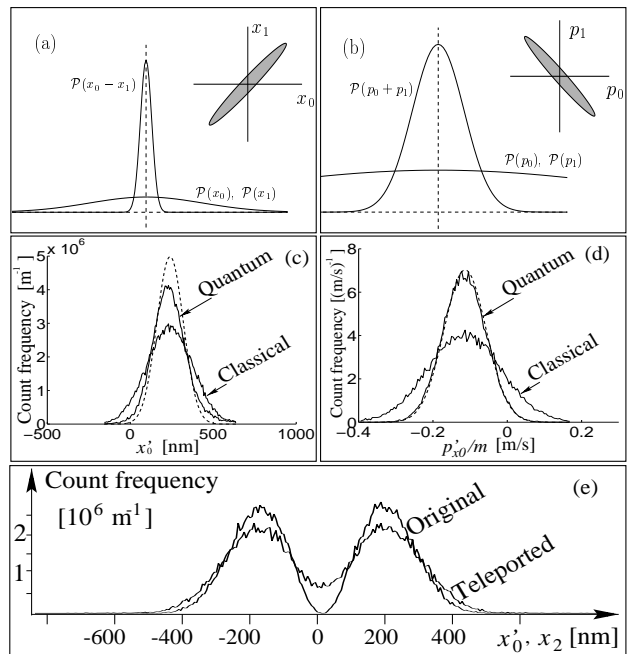


FIG. 2. Probability distributions of the separation $\mathcal{P}(x_0 - x_1)$ (a) and momentum-sum $\mathcal{P}(p_0 + p_1)$ (b) of the EPR pair, as compared with their respective single-particle counterparts $\mathcal{P}(x_{0(1)})$ and $\mathcal{P}(p_{0(1)})$. (c)-(e): Our prediction for the results of 5×10^4 teleportation events with lithium ions with the parameters as in the text. (c) position, and (d) momentum distribution of a Gaussian wavepacket, broken line: ideal input distributions, full lines: results of classical and quantum teleportations (by following classical trajectories of an ensemble obeying the quantum Wigner $x - p$ distribution). (e): Prediction of the teleported position distribution of a two-peak interference pattern (by applying the calculated teleportation-induced noise to the input distribution).

We suggest that the translationally-entangled particles 0 and 1 can be used to demonstrate the *hitherto unobserved* original prediction of EPR [8], concerning the nonlocality of quantum correlations in a free-propagating two-atom state satisfying inequality (1): detecting the momentum or position of particle 1 would make the corresponding variable of particle 0 assume a nearly well-defined value (with fluctuations \hbar/D or Δd , respectively). By contrast, there will be large fluctuations if we measure *uncorrelated* variables (Fig. 2 (a), (b)): the momentum of particle 1 and the position of particle 0, or vice versa. We note that the preparation of EPR states of *internal atomic observables* (unlike the present external or translational observables) by diatomic dissociation was discussed in [12,13] (for atomic excitations or pseudospin states), and in [14] (for atomic spin states). An EPR correlation of *trapped* (rather than free-propagating) atoms is proposed in [15].

The major challenge is to teleport the quantum state

$|\psi_{in}\rangle$ of the *transversal* motion of particle 2 (along the x axis) to particle 0 (Fig. 1). To this end, particle 2 collides with one member of the EPR pair – particle 1 (in a synchronous fashion determined by laser pulses—see below), after which both particles 1 and 2 are detected. Essentially, the collision of particles 1 and 2 allows us to project their pre-collisional *joint state* onto the basis of EPR-correlated states (specified below) and detect the result of the projection. The results of the post-collision detection are used to control the evolution of the “read-out” particle 0, the other member of the EPR pair. In the optimal case, the resulting translational state $|\psi_{out}\rangle$ of particle 0 would closely imitate the input $|\psi_{in}\rangle$ of particle 2. We may assume that $|\psi_{in}\rangle$ is prepared by diffraction on a double-slit screen or grating [16]. If measured directly, the beam of particle 2 would exhibit a characteristic diffraction pattern. If the teleportation scheme is applied instead, then the input beam is destroyed but nearly the same diffraction pattern can be observed in the transformed output beam of particle 0. We note that the collision region in Fig. 1 plays an *analogous role to the beam-splitter* which mixes a field quadrature of the teleported optical state with the field of one of the entangled PDC modes in the teleportation scheme of [5].

A natural choice for the post-collision correlated (EPR-state) basis is the set of states associated with a sharp (well-defined) sum of the colliding particles’ momenta $\hat{p}_{x1} + \hat{p}_{x2}$ and sharp difference of their x coordinates, $\hat{x}_1 - \hat{x}_2$. At the time instant τ , corresponding to the particles’ nearest approach in the absence of interaction (see below), the operators \hat{x}_- and \hat{p}_+ , given by

$$\hat{x}_- \equiv \hat{x}_1(\tau) - \hat{x}_2(\tau) \quad (3)$$

$$\hat{p}_+ \equiv \hat{p}_{x1}(\tau) + \hat{p}_{x2}(\tau) \quad (4)$$

are measured, with values x_-, p_+ and precision Δx_{meas} and Δp_{meas} , respectively (which are discussed below).

The last step required for the teleportation of the state of particle 2 is the shift of the x -coordinate and momentum of the “readout” particle 0, according to the inferred values of x_- and p_+ as $\hat{x}_0 \rightarrow \hat{x}'_0 = \hat{x}_0 - x_-$, and $\hat{p}_{x0} \rightarrow \hat{p}'_{x0} = \hat{p}_{x0} + p_+$. Let the precision of the position and momentum shifters be Δx_{shift} and Δp_{shift} , respectively. From the correlations of \hat{x}_0 and \hat{x}_1 , or \hat{p}_{x0} and \hat{p}_{x1} discussed above, we find that (at the relevant times) the shifted variables satisfy

$$\hat{x}'_0 = \hat{x}_2 \pm \Delta x_T, \quad (5)$$

$$\hat{p}'_{x0} = \hat{p}_{x2} \pm \Delta p_T, \quad (6)$$

namely, they approximately *reproduce the teleported variables of particle 2*, to the accuracy given by Δx_T and Δp_T where

$$\Delta x_T^2 = \Delta d^2 + \Delta x_{\text{meas}}^2 + \Delta x_{\text{shift}}^2, \quad (7)$$

$$\Delta p_T^2 = \Delta P_x^2 + \Delta p_{\text{meas}}^2 + \Delta p_{\text{shift}}^2. \quad (8)$$

Equations (5), (6) imply that the Wigner $x - p$ distribution $W(x'_0, p'_{x0})$ of the readout particle 0 is given by

that of the input particle 2, $W_{in}(x_2, p_{x2})$, coarse-grained by a smoothing function whose width is determined by Eqs. (7), (8).

The teleportation has non-classical properties provided: (i) Δx_T and Δp_T satisfy

$$\Delta x_T \Delta p_T < \hbar; \quad (9)$$

(ii) they are finer than the scales of the input wavepacket variation in position and momentum, respectively [Fig. 2(c)-(e)]. If the fluctuations produced by the measurements and shifts are negligible ($\Delta x_{\text{meas}}, \Delta x_{\text{shift}} \ll \Delta d$, and $\Delta p_{\text{meas}}, \Delta p_{\text{shift}} \ll \Delta P_x$), then the left-hand side of Eq. (9) is approximately $\Delta x_T \Delta p_T \approx \hbar/s$. For teleported Gaussian wavepackets, the maximum attainable fidelity, i.e., the overlap of the input state with the teleported output, can be shown to be $F_{\text{max}} = (1 + \Delta x_T \Delta p_T / \hbar)^{-1}$. As shown in [5], the maximal *classical* teleportation fidelity is 1/2, so that larger fidelity, as in the quantum-optical teleportation experiment [6] where $F = 0.58$, attests to quantum correlations. [“Classical teleportation” is based on simultaneous (though noisy) measurements of the non-commuting quantities \hat{x}_2 and \hat{p}_{x2} and preparing a corresponding MUS wavepacket of particle 0.]

We proceed to discuss the experimentally relevant aspects of the envisaged teleportation. The dissociated pairs of fragments (particles) 0 and 1 can be emitted in all directions, but the dissociating field polarization can impose directionality [17]. A significant fraction of the fragment pairs enter the aperture of the lens focussing them onto the region where the collision of particles 1 and 2 takes place. The colliding particles are assumed to be prepared in *uncorrelated* wavepackets propagating with the same classical velocity along z , $v_{z1} = v_{z2}$, and opposite classical momenta along y (Fig. 3), $m_1 v_{y1} = -m_2 v_{y2}$, such that $v_{z1,2} \gg |v_{y1,2}| \gg \Delta v_{x1,2}$. Their focussing (and laser-pulse deflection) is such that *in the absence of interaction* the wavepackets would cross each other in the xy plane, where their size would be smallest (“contractive” wavepackets [18]). Let us take both particles 1 and 2 to be equally charged. Charged-particle focussing (by electrostatic and magnetic lenses used in high-resolution microscopy) would render the spread (“spot size”) of the colliding particles’ positions as sharp as it was at the relevant times (thus achieving “time-reversal”): for particle 1 this time corresponds to the completion of dissociation, whereas for the teleported particle 2 it is the time of the state preparation (e.g., by a double slit). The arrival of the two particles in the xy collision plane at τ must be *synchronized by laser pulses*, causing the fast switching-on of their deflection towards the collision region in the $x - y$ plane, provided the values of $z_1, z_2, v_{z1} = v_{z2}$ are appropriate. Synchronization accuracy of ~ 10 ps and $v_z \sim 10^3$ m/s would bring the particles well within the Coulomb collision range (see below). The $y - z$ extent of the two wavepackets must be $\Delta d_c \ll D$, so that they overlap in the absence of Coulomb repulsion

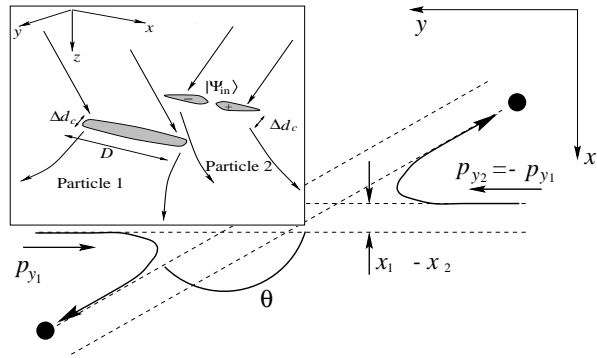


FIG. 3. Collision scheme of particles 1 and 2. Their deflection angle θ corresponds to the collision distance $x_1 - x_2$. Their momentum sum is conserved. Inset: structure of wavepackets 1 and 2, marked by width Δd_c along the y and z axes and carrying quantum information along the x axis.

(Fig. 3–inset). Among the dissociated atom pairs entering the input aperture L , only those participating in the *synchronized* collision events are counted as pairs that contribute to successful teleportation.

The success of teleportation hinges upon our ability to discriminate, when detecting the post-collision states, between correlated EPR states with *different values of the relevant parameters*, namely, the parameter x_- and the momentum sum p_+ in Eqs. (3) and (4). We can infer the parameter x_- by measuring the relative deflection angle of the colliding particles. A quantitative estimation can be made for repulsive Coulomb interaction of two particles with mass m and charge q . Their relative deflection angle is given by (see, e.g., [19]) $\theta = \pi - 2 \tan^{-1} [(x_1 - x_2)/R_{\text{col}}]$, where $R_{\text{col}} = mq^2/(4\pi\epsilon_0 p_y^2)$ is the characteristic collision range. To ensure maximal sensitivity of the deflection angle to x_- it is useful to choose the experimental parameters such that $\Delta d_c \ll R_{\text{col}} \sim D \sim \max|x_-|$. From the collisional analysis it follows that the precision of inferring x_- is mostly affected by the fluctuation of its conjugate momentum component $\Delta(p_{x2} - p_{x1}) \sim \hbar/\Delta d_v$. The corresponding resolution of x_- , obtained from that of θ , is $\Delta x_{\text{meas}} \approx \pi\epsilon_0 \hbar D^2 p_y / (2q^2 m \Delta d_v)$, provided that $p_y \gtrsim \sqrt{mq^2/(4\pi\epsilon_0 D)}$. In particular, for lithium ions with velocities $v_y \approx 300$ m/s, $R_{\text{col}} \approx 220$ nm, the resolution of position difference measurements is $\Delta x_{\text{meas}} \approx 15$ nm. The momentum-sum p_+ is measurable by the Doppler shift of Raman transitions induced by two counterpropagating laser fields, with precision better than 1 mm/s [20]. The dominant contribution to its resolution, Δp_{meas} , then stems from the fluctuation ΔP_x , which is, for the given parameters, $\Delta P_x/m \approx 30$ mm/s.

In the last stage of teleportation, particle 0 must be “kicked” (momentum-shifted) and position-shifted by external fields. The spread incurred by these shifts is incorporated into Eqs. (7) and (8), and constitutes one of the factors in the anticipated resolution used in the tele-

portation simulations of Fig. 2(c). Yet the precision of ion optics is currently so high that the dominant contributions in Δx_T and Δp_T stem from Δx_{meas} and Δp_{meas} , respectively. We then get for the teleportation of lithium ion wavepackets, under the conditions specified above, the estimation $\Delta x_T \Delta p_T / \hbar \approx 0.08 \ll 1$. Such spreads would allow for much higher teleportation fidelities of continuous variables than those presently achievable in quantum optical experiments.

The foregoing analysis shows that, despite the challenging nature of the proposed ideas, their experimental implementation does not pose insurmountable (rather than technical) difficulties. The teleportation of matter wavepackets by molecular dissociation and collisions is a novel concept, combining elements of molecular dynamics and ion (atom) optics, and having quantum optical analogues. Its realization is a challenging but viable goal to pursue, en route to quantum information exchange between complex material objects.

Acknowledgments: The support of US-Israel BSF and DFG is acknowledged. G. K. holds the G. W. Dunne Professorial Chair.

-
- [1] C. Bennett et al., Phys. Rev. Lett. **70**, 1895 (1993).
 - [2] L. Vaidman, Phys. Rev. A **49**, 1473 (1994).
 - [3] D. Bouwmeester et al., Nature **390**, 575 (1997).
 - [4] D. Boschi et al., Phys. Rev. Lett. **80**, 1121 (1998).
 - [5] S. L. Braunstein and H. J. Kimble, Phys. Rev. Lett. **80**, 869 (1998).
 - [6] A. Furusawa et al., Science **282**, 706 (1998).
 - [7] A. Kuzmich and E. S. Polzik, Atomic quantum state teleportation and swapping. arXiv: quant-ph/0003015 (2000).
 - [8] A. Einstein, B. Podolsky, and N. Rosen, Phys. Rev. **47**, 777 (1935).
 - [9] R. Wynar et al., Science **287**, 1016 (2000).
 - [10] M. D. Reid and P. D. Drummond, Phys. Rev. Lett. **60**, 2731 (1988).
 - [11] Z. Y. Ou et al., Phys. Rev. Lett. **68**, 3663 (1992).
 - [12] G. Kurizki and A. Ben-Reuven, Phys. Rev. A **32**, 2560 (1985).
 - [13] G. Kurizki, Phys. Rev. A **43**, R2599 (1991).
 - [14] E. S. Fry, T. Walther, and S. F. Li, Phys. Rev. A **52**, 4381 (1995).
 - [15] A. S. Parkins and H. J. Kimble, Phys. Rev. A **61**, 2104 (2000).
 - [16] S. Kunze, K. Dieckmann, and G. Rempe, Phys. Rev. Lett. **78**, 2038 (1997).
 - [17] J. J. Larsen et al., Phys. Rev. Lett. **83**, 1123 (1999).
 - [18] P. Storey et al., Phys. Rev. A **49**, 2322 (1994).
 - [19] B. H. Bransden, Atomic Collision Theory 2nd ed. (Benjamin/Cummings, Reading, Massachusetts, 1983).
 - [20] M. Kasevich, et al. Phys. Rev. Lett. **66**, 2297 (1991).